

Microstructure similarity analysis between synthetic phase-separated block copolymers and natural spider silk

Qin Yang

School of materials science and engineering, China University of Geosciences,
Beijing, China, 518000.

YOLO-QFTN@outlook.com

Abstract. This paper's primary purpose is to explore why the microstructure of synthetic block copolymers and natural spider silk is similar at the nanoscale. This paper analyses the main chain segments and secondary structures of natural spider silk, clarifies the aggregation order, and introduces the contribution of secondary systems to the properties of natural block copolymers. Secondly, combined with the synthesis mechanism of natural spider silk, this paper summarizes and analyzes the general process of the synthesized block copolymer. Finally, the conditions of self-assembly of artificial fragments to form the structure are analyzed by employing mean-field theory and a phase diagram. Natural and ideal synthetic spider silk block copolymers have high similarity in performance. To achieve this, scientists can only start from the primary segment to understand their arrangement order in the secondary structure. Then the influence of each block on the properties of the silk fiber is analyzed. At the same time, the size and shape of self-assembled block copolymers are controlled at the micro-scale, thereby changing their properties. The mechanism above shows that the synthesized spider silk block copolymer is similar to natural spider silk in microscopic morphology.

Keywords: Block copolymers, Spider silk, Micro-phase separation, Self-assembly, Microstructure.

1. Introduction

Many natural biological materials have excellent and environmentally friendly characteristics, which make various research fields learn from and simulate their structures. Zhang et al. used agricultural solid wastes such as rice straw to simulate and synthesize a beetle-like octopus wing plate structure. This 3D microstructural structure is a highly evolved design with excellent performance, combining the characteristics of lightness, strength, and camouflage [1]. Spider silk has excellent comprehensive properties that are unmatched by any other fiber. Its specific strength is five times that of steel, and its elasticity is ten times that of aramid fiber. More importantly, it also has the highest fracture toughness of all materials [2-5]. Spider silk fibers also showed a special torsional shape memory effect. When suspended in the air, the silk fibers allow the spider to spin around and move up and down without shaking. No matter how the spider spins, the thread is instantly restored to its original state[6].

At the nanometer scale, this paper explores the following content:

1. Analyze the primary segments and secondary structures of natural silk.
2. Clarify the polymerization orders and the microstructures of each secondary structure.

3. A summary of the contribution of each microstructure to the performance of natural block copolymers.
4. Summary and analysis of the general process of the synthesized block copolymers according to the synthesis mechanism of natural spider silk.
5. Utilizing the mean-field theory and phase diagram, the paper analyzes the conditions of artificial fragment self-assembly to form a structure.

By analyzing the self-assembly conditions of synthetic block copolymers, a theoretical analysis method is provided for the further design of block copolymers with different shapes and functions to face more applications. It is worth mentioning that exploring how to synthesize block copolymers similar to natural spider silk under mild conditions may be of great help to developing the properties of synthetic silk to the maximum extent.

2. Primary and secondary structures of natural spider silk block copolymers

Spider silk is tailored for specific purposes and shows tremendous differences in mechanical properties. There are significant differences in the performance of spider silk for different purposes. Of course, this stems from the difference in their microstructure. The strength (breaking stress) of different types of spider silk is between 0.02-1.7 GPa, indicating that the power of some types of silk even exceeds that of steel (1.5 GPa). Their flexibility is also very different, in the range of 10%-500% [7].

Spider silk is a natural block copolymer, as shown in Figure 1. Take the golden globe weaver spider, *N. clavipes*, as an example. Their ampulla glands can produce a kind of traction silk with high tensile strength and high flexibility, which is used to form the framework of spider webs and help spiders hang [7-8]. This filament mainly comprises major ampullary dragline protein 1 (MaSp1) and major ampullary dragline protein 2 (MaSp2). Different spiders have different ratios of MaSp1 and MaSp2, meaning different silk fibers' properties[9]. Among them, the primary small peptide motifs of different types of MaSp1 include these three types: poly(A/GA), glycine-rich domain (GGX), and non-repetitive N- and C- termini[10].

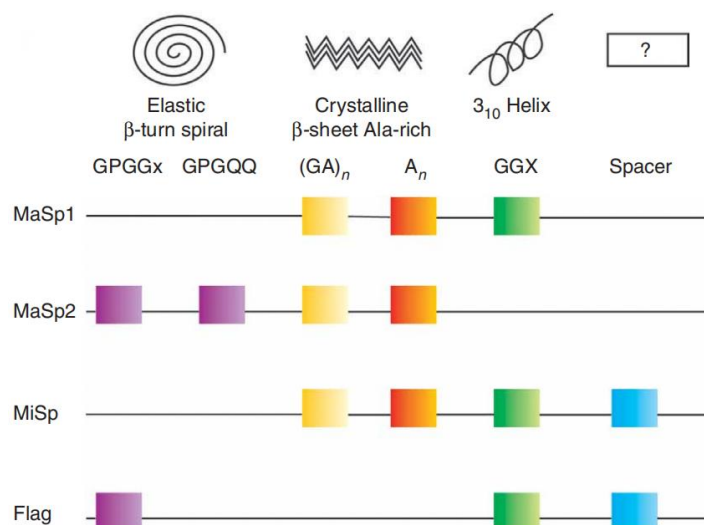


Figure 1. Major secondary structures and their primary fragment arrangement; Reprinted from Ref. with permission [11].

Araneus diadematus spider produces ADF-3 and ADF-4, similar to MaSp1 and MaSp2 proteins, respectively, with similar structural sequences and functions[12]. It is worth noting that they do not aggregate in the spider body but are separately stored in capsules with different lumens in the form of high concentration liquid (molecular weight > 200 kDa). As seen in Figure 2, spiders will expose proteins to specific chemical and mechanical stimuli to assemble proteins into fibers when necessary. Interestingly, their distribution in spider silk fibers is not uniform[13].

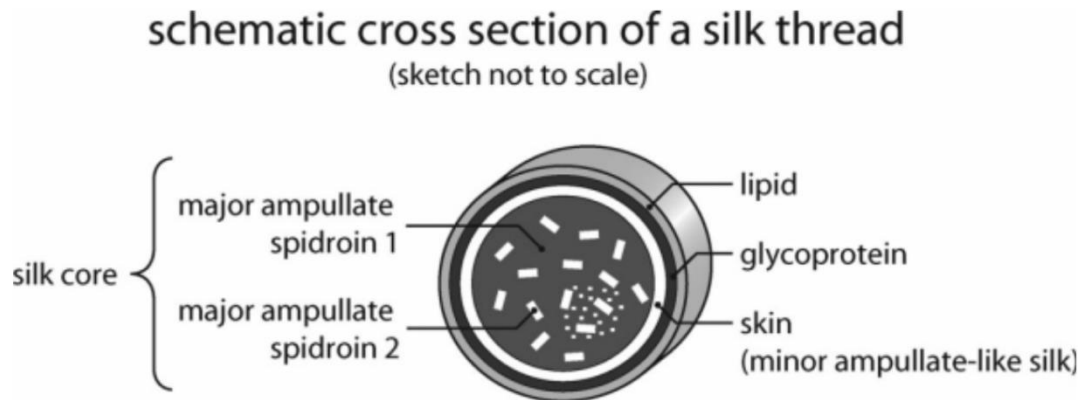


Figure 2. Diagram of main ampullary filament cross-section; Reprinted from Ref. with permission [14].

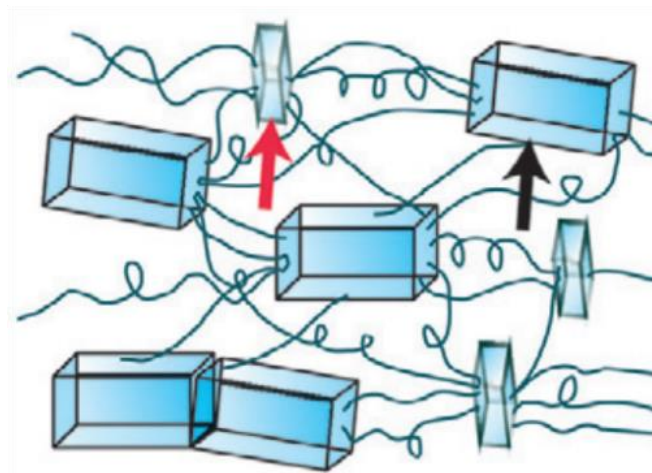


Figure 3. Spider silk fibers include tiny, tightly packed β -sheet crystals (the red arrow) and crystalline regions (the black arrow), as well as a soft amorphous matrix; Reprinted from Ref. Permission[15].

The prominent physical properties of the significant ampulla traction filaments are derived from the primary protein sequence. The primary structure of the spider ligand is a highly repetitive intermediate domain. It is composed of alternating polyalanine (Polygala), glycine-rich fragments, and C- and N-terminal parts. Figure 3 shows alternating polyalanine (Polygala) assembled into an antiparallel β -Sheet secondary structure. It forms a crystal domain in spider silk and gives the silk fiber high tensile strength. The glycine-rich fragment is mainly composed of the GGX (G: Glycine; X: leucine, tyrosine, or glutamine) motif and several other residues such as serine or valine. Their softness gives the spider traction on silk elasticity [16].

Most spider silk generally consists of four different motifs(see 0): (I) 3_{10} -helices form the repeat GXX; (II) crystalline β -sheet rich poly(A) / poly(GA) motifs; (III) an elastic beta-spiral region, also known as proline-rich region, composed of multiple GPGXX motifs; (IV) a spacer region with unknown functions[16]. The interaction between the motif rich in amino acids and GA greatly impacts the secondary structure of silk proteins. Different interactions form secondary structures, affecting spider silk's physical properties and promoting silk fibers' rapid formation(see 0[9, 15, 17].






Structure	Illustration	Amino acid sequence
random coil		various
α -helix		NR_N / NR_C regions and A_n (in solution)
3_{10} -helix		(GGX)
β -sheet		$(GA)_n / A_n$
β -turn		(GPGQQ) / (GPGGX)

Figure 4. Secondary structure motifs in spider silk block copolymers; Reprinted from Ref. with permission [17].

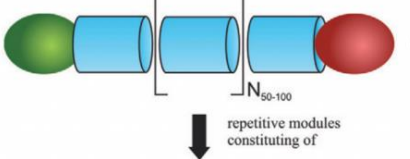
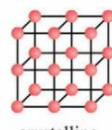




<div style="display: flex; align-items: center; justify-content: space-around;"> <div>non-repetitive amino-terminal domain</div>  <div>non-repetitive carboxy-terminal domain</div> </div> <div style="text-align: center; margin-top: 10px;"> repetitive modules constituting of </div>						
protein \ sequence motif	(A) ₄₋₁₃	(GA) ₄₋₆	GGX	GPGXX	Spacer	Termini
Major ampullate Spidroin 1 (MaSp1)	✓		✓			✓
Major ampullate Spidroin 2 (MaSp2)	✓			✓		✓
Minor ampullate Spidroins (MiSp)		✓	✓		✓	✓
Flagelliform spidroin (Flag)			✓	✓	✓	✓
Araneus Diadematus Fibroin 3 (ADF3)	✓		✓	✓		✓
Araneus Diadematus Fibroin 4 (ADF4)	✓			✓		✓
structural role	 crystalline	 amorphous	 elastic	 spacer	 storage & assembly	

Figure 5. Secondary structures contained in several spider silk proteins and their contribution to fiber properties; Reprinted from Ref. with permission [15].

3. Design and assembly of synthetic spider silk block copolymer

Scientists designed and assembled a series of synthetic spider silk block copolymers based on analyzing the primary and secondary structures of natural spider silk block copolymers. Among them, polyaniline and glycine-rich domains have been studied more, and they will show different phase behaviors in the

aqueous solution, which is also the focus of the analysis [18-19]. Examples include the design and synthesis of a block copolymer with a unique sequence structure similar to spider silk protein.

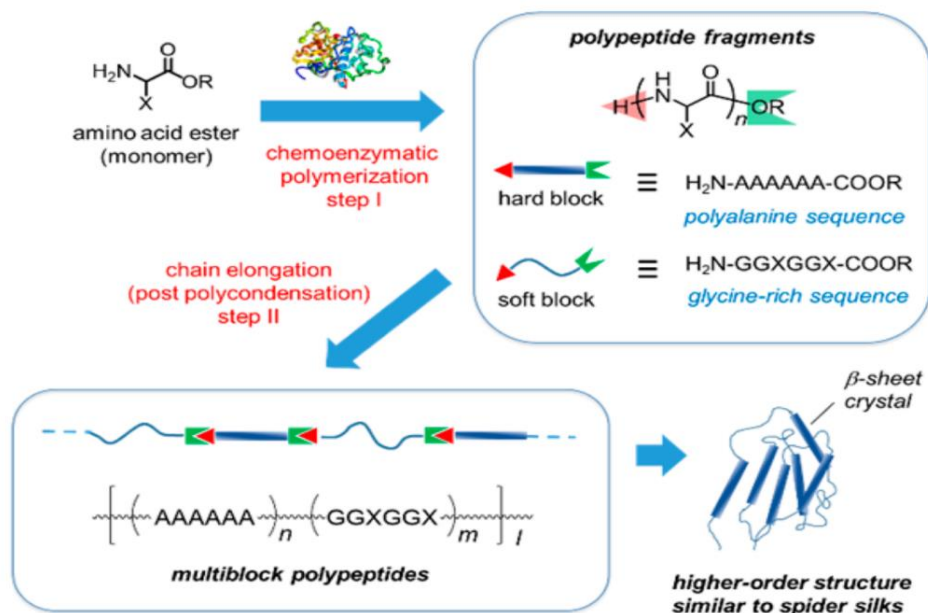


Figure 6. A method for synthesizing the microstructures resembling spider silk proteins, the resultant block copolymers have β -sheets and a soft amorphous matrix; Reprinted from with permission [20].

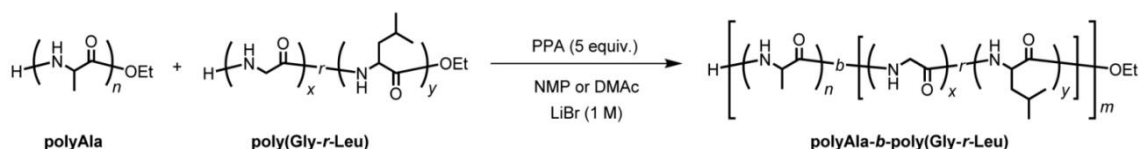


Figure 7. Specific condensation reaction equations for polyalanine and glycine-rich fragments; Reprinted from with permission [20].

Figure 6 and Figure 7 show that the two-step synthesis process prepares spider filament-like multiblock peptides. Oligopeptide fragments are similar in sequence to spidroins, namely hard polyAla and soft glycine-rich fragments. The two peptides were polymerized using papain to form a polymeric structure similar to that found in spider silk fibrin. PolyAla forms β -sheet structures, while poly (glycine-random leucine) forms the soft segments between PolyAla sequences which is similar to the spidroin repeat domains. Soft segments are rich in glycine and help spider silk stretch. The polymerization was carried out in phosphate buffer/methanol at 40°C and pH 8.0 and precipitated by centrifugation to give a white powdered polylactic acid [20].

4. Microphase separation of self-assembled spider silk block copolymers

In this step, employing the mean-field theory and phase diagram (see Figure 8), it is possible to analyze the conditions for the self-assembly of the dragline filament (genetic variant HBA-HBA6) of the main ampulla of the spider (*N. clavipes*) to form the tissue structure. Region a (hydrophobicity) is represented by polyalanine repeats. The B region (hydrophilic) consists of GGX repeats. The H region (histidine tag) consists of six residues and a short linker sequence. The effects of purified tags and linker sequences on small peptide fragments need not be considered [21].

Flory–Huggins equation for the Gibbs free energy is as follow:

$$\Delta G_m = k_B T (N_1 \ln \phi_1 + N_1 \ln \phi_2 + N_1 \phi_2 \chi_1) \quad (1)$$

(k_B is the Boltzmann constant. ϕ_i is the percentage of occupied sites.)

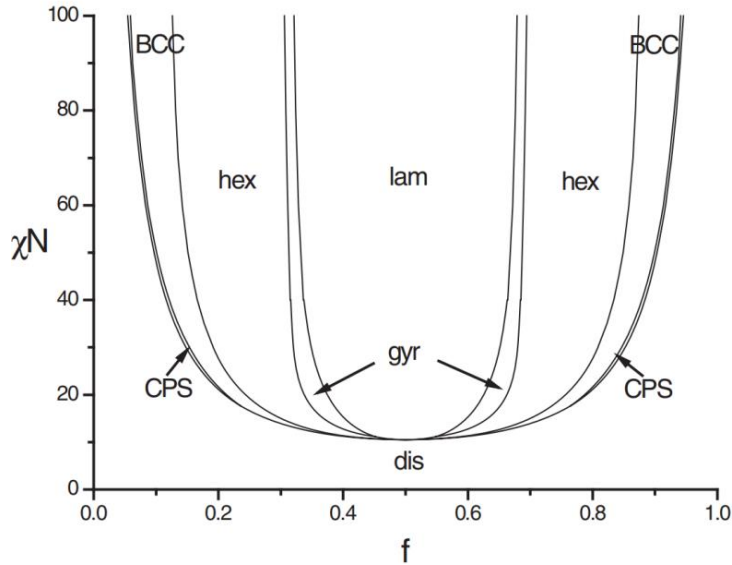


Figure 8. Schematic phase diagram of “AB” block copolymers. (f is the volume fraction of one of the blocks, χ is the Flory — Huggins interaction parameter between A and B, and N is the total polymerization degree of the block copolymer); Reprinted from Ref. with permission [22].

As can be seen from the above phase diagram, block copolymer self-assembly into the tendency of ordered phase form depends on the strength of the mutual repulsion between each block, expressed with χN , which is suitable for block AB χ Florida — between Huggins (Flory Huggins) interaction parameter, N polymerization degree in total for block copolymer. When this value exceeds the critical value of the order-disorder transition, the microphase separation will occur. The control block copolymer microphase separation is one of the important parameters χN , when $\chi N \leq 10$, weak phase separation occurred; When $\chi N \geq 10$, strong phase separation occurred. AB type deblock copolymers solutes form different ordered structures according to the volume fraction of A monomer (the ratio of the length of A block to the total length of two blocks). When the volume fraction is small, block A forms microdomains, and block B forms matrixes. When large, block B forms microdomains, and block A forms matrixes. According to the mean-field theory, in order to make f_A achieve 0.50, increasing N over 10.5 is required to form ordered structures (e.g., lamellar)[23].

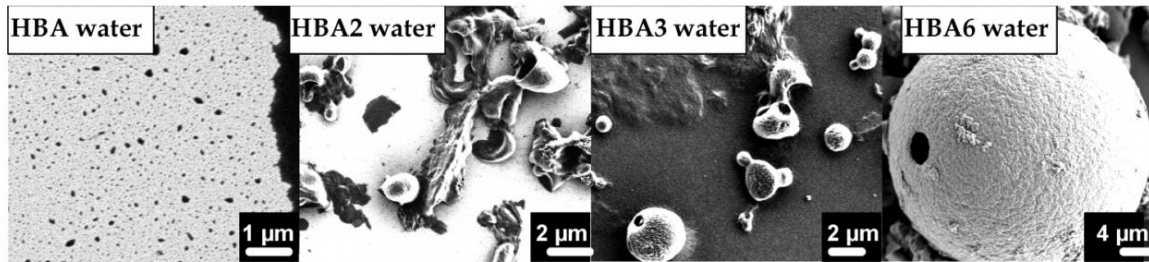


Figure 9. Molecular self-assembly process of synthetic block copolymers with different contents of trap fragments in water; Reprinted from Ref. with permission [21].

As can be seen from Figure 9, since the fA of HBA block copolymers is 14%, which does not meet the required value of χ N (it controls the degree of separations), which means tiny fragments are in disorder. HBA2(fA is calculated to be 26%) assembles itself into micelles which are bowl-shaped with an overall 1-3 μ m in diameter. When fA increased to 36%(HBA3), the granules gradually became spherical and then began to appear as tiny, short fibers. When fragment A multiplies to 6, at which time fA exceeds 50%, small spherical colloidal particles assemble to form large colloidal particles with diameters between 30 and 70 microns. It is worth mentioning that these large spherical colloidal particles have holes as long as 25 nanometers in diameter[21].

It was found that the tendency of the self-assembly behavior of block copolymers to change into specific morphology is linearly related to the quantity of hydrophobic blocks(A). The augment of hydrophobic blocks changes the self-assembly behavior of block copolymers in both morphology and microstructure. On the one hand, with the increase of hydrophobic blocks, block copolymers gradually assemble into micelles(1-3 μ m) from thin films and finally into giant compound micelles(50 μ m)[21]; On the other hand, with the increase of block A, the proportion of β -sheet in silk fiber block copolymers scale up.

5. Conclusion

The main reason the microstructure of synthesized block copolymers and natural spider silk are similar is that their primary and secondary structures are identical. The conditions of their microstructure self-assembly are also similar. The secondary structures of the synthesized block copolymers and the natural silk block copolymers are mainly polyalanine repeats, GGX repeats, etc. Spider silk protein is stored separately in capsules in the body of spiders as complex micellar nanoparticles composed of aggregated secondary structures. This high-concentration storage form is complicated for scientists to imitate before being extruded from the body. It is also an important reason that limits the microstructure difference between the synthetic spider silk block copolymer and the natural spider silk and directly leads to the performance difference between them. Therefore, it is crucial to deeply understand the assembly of nanoscale proteins to mimic the microstructure and properties of natural silk greatly. Through the analysis of the reasons for the microstructure similarity between the synthetic and natural spider silk block copolymers, we can clearly see the differences in the arrangement of the primary fragments of the two of them and the differences in the synthesis conditions and catalysts at the nanometer scale, and can quickly find the reasons for the differences in their performance: On the one hand, the synthetic block copolymers are only formed by simple repetitive alternating polymerization of several primary, secondary structures, and do not contain some unknown functional regions. On the other hand, unlike natural block copolymers, which are stored separately in a highly concentrated form in spiders and temporarily and efficiently form silk fibers when they are extruded, synthetic block copolymers are formed in experimental vessels after a series of long-time operations.

Therefore, to make the shape, material, and properties of the synthetic block copolymer more similar to natural spider silk, scientists can start with the above two aspects. In addition, the analysis and conclusions presented in this paper are based on existing research and experimental data, which have certain limitations. More specific experimental operations and phenomena are needed for further exploration.

6. Acknowledgments

I completed this article under the careful guidance of my professor and teachers. When selecting the topic and listing the outline, the professor took time out of his busy schedule to help me analyze and guide my thoughts. Although the professor pointed out that my draft was off-topic at that time, it made me stop losing in the wrong direction. I admire his rigorous and careful attitude towards research, which has profoundly impacted me. At the same time, I am also very grateful to my teaching assistant. When I was confused about the research direction or even about to collapse, he made a temporary appointment to patiently teach me how to analyze documents. He has helped me make significant progress in learning how to deal with a large number of English documents efficiently. In addition, I am also grateful to the

other teachers in charge of this project. Without their attention and supervision, I could not finish this paper well. Finally, I thank my family for supporting me during this period. Although they can't help me in my study, they always give me enough care whenever I need to improve. In short, I am very grateful to the people who cared about me and guided me during my growing up. I am fortunate to have them to enlighten my present and future.

References

- [1] Zhang Z, Chen J, Elsafi M E, et al. (2018). Effects of changes in the structural parameters of bionic straw sandwich concrete beetle elytron plates on their mechanical and thermal insulation properties[J]. *Journal of the Mechanical Behavior of Biomedical Materials*, 90.
- [2] LEWIS R V. (2006). Spider silk: ancient ideas for new biomaterials[J]. *Chemical reviews*, 106(9): 3762-3774.
- [3] Vollrath, F., & Porter, D. (2006). Spider silk as archetypal protein elastomer. *Soft Matter*, 2(5), 377-385.
- [4] Heim, M., Keerl, D., & Scheibel, T. (2009). Cheminform abstract: spider silk: from soluble protein to extraordinary fiber. *Angewandte Chemie International Edition*, 40(28), 3584-3596.
- [5] Gosline JM, Guerette PA, Ortlepp CS, Savage KN. (1999). The mechanical design of spider silks: from fibroin sequence to mechanical function. *J Exp Biol* 202:3295–3303.
- [6] Emile, O., Le Floch, A., & Vollrath, F. (2006). Shape memory in spider draglines. *Nature*, 440(7084), 621-621.
- [7] Swanson, B. O., Blackledge, T. A., Summers, A. P., & Hayashi, C. Y. (2006). Spider dragline silk: correlated and mosaic evolution in high-performance biological materials. *Evolution* 60(12), 2539-2551.
- [8] Heim, M., Keerl, D., & Scheibel, T. (2009). Spider silk: from soluble protein to extraordinary fiber. *Angewandte Chemie*, 48(20), 3584-3596.
- [9] Tokareva O, Jacobsen M, Buehler M, et al. (2014). Structure-function-property-design interplay in biopolymers: Spider silk[J]. *Acta Biomaterialia*, 10(4):1612-1626.
- [10] Xu, M., & Lewis, R. V. (1990). Structure of a protein superfiber: spider dragline silk. *Proceedings of the National Academy of Sciences*, 87(18), 7120-7124.
- [11] Teulé, F., Cooper, A. R., Furin, W. A., Bittencourt, D., Rech, E. L., Brooks, A., & Lewis, R. V. (2009). A protocol for the production of recombinant spider silk-like proteins for artificial fiber spinning. *Nature protocols*, 4(3), 341-355.
- [12] Scheibel T. (2012). Production and Processing of Spider Silk Proteins[J]. *GAK Gummi Fasern Kunststoffe*, 65(1):41-43.
- [13] Parent, L. R., Onofrei, D., Xu, D., Stengel, D., Roehling, J. D., Addison, J. B., ... & Holland, G. P. (2018). Hierarchical spidroin micellar nanoparticles as the fundamental precursors of spider silks. *Proceedings of the National Academy of Sciences*, 115(45), 11507-11512.
- [14] Eisoltd, L., Smith, A., & Scheibel, T. (2011). Decoding the secrets of spider silk. *Materials Today*, 14(3), 80-86.
- [15] *Journal of Polymer Science Part A-Polymer Chemistry*[J]. (2008). *Materials Chemistry and Physics*, (112): 551-556.
- [16] Gu Y, Yu L, Mou J, et al. (2020). Mechanical properties and application analysis of spider silk bionic material[J]. *E-Polymers*, 20(1):443-457.
- [17] Zhao, J., Zhang, G., & Pispas, S. (2009). Morphological transitions in aggregates of thermosensitive poly(ethylene oxide)-b-poly (N-isopropylacrylamide) block copolymers prepared via RAFT polymerization. *Journal of Polymer Science Part A: Polymer Chemistry*, 47(16), 4099-4110.
- [18] Rabotyagova, O. S., Cebe, P., & Kaplan, D. L. (2009). Self-assembly of genetically engineered spider silk block copolymers. *Biomacromolecules*, 10(2), 229-236.
- [19] Rabotyagova, O. S., Cebe, P., & Kaplan, D. L. (2010). Role of polyalanine domains in β -sheet formation in spider silk block copolymers. *Macromolecular bioscience*, 10(1), 49-59.

- [20] Kousuke Tsuchiya, Keiji Numata. (2018). Chemical Synthesis of Multiblock Polypeptides Inspired by Spider Dragline Silk Proteins[J]. ACS Macro Letters. 6(2):103-106.
- [21] Rabotyagova, O. S., Cebe, P., & Kaplan, D. L. (2009). Self-assembly of genetically engineered spider silk block copolymers. Biomacromolecules, 10(2), 229-236.
- [22] Wyss, H. M. (2013). Fundamentals of Soft Matter Science. Physics Today, 66(11), 50.
- [23] Fredrickson, G. H., & Bates, F. S. (1996). Dynamics of block copolymers: Theory and experiment. Annual Review of Materials Science, 26(1), 501-550.